Int. J. Anal. Appl. (2026), 24:2

International Journal of Analysis and Applications

Fractal-Fractional Modeling and Analysis of Monkeypox Disease Using Atangana-Baleanu Derivative

Tharmalingam Gunasekar[1,2,3,*], Shanmugam Manikandan[1], Murgan Suba[4], Irshad Ayoob[5], Nabil Mlaiki[5,*]

[1]*Department of Mathematics, Vel Tech Rangarajan Dr. Sagunthala R&D Institute of Science and Technology, Chennai-62, Tamil Nadu, India*

[2]*School of Artificial Intelligence & Data Science, Indian Institute of Technology (IIT), Jodhpur, Rajasthan, India*

[3]*Department of Mathematics, Srinivas University, Mukka, Mangaluru - 574146, Karnataka, India*

[4]*Department of Mathematics, S.A. Engineering College (Autonomous), Chennai-77, Tamil Nadu, India*

[5]*Department of Mathematics and Sciences, Prince Sultan University, Riyadh 11586, Saudi Arabia.*

[*]*Corresponding author:* tguna84@gmail.com; nmlaiki@psu.edu.sa

Abstract. In this study, we formulate a deterministic mathematical model to describe the transmission dynamics of the monkeypox virus using fractal and fractional-order differential equations. The model incorporates all possible interactions influencing disease propagation within the population. Our analysis primarily focuses on the stability of fractal–fractional derivatives, aiming to establish the existence and uniqueness of solutions through the fixed-point theorem. Additionally, we examine Ulam-Hyers stability and other significant findings related to the proposed model. To enhance numerical accuracy, we employ Lagrange polynomial interpolation for computational approximations. Finally, graphical simulations for various fractal–fractional orders are presented to validate the model's effectiveness and demonstrate its practical relevance.

1. Introduction

In 1958, introducing two Cynomolgus monkeys from Singapore to Copenhagen resulted in a smallpox-like outbreak among the monkeys. Outbreaks were discovered in captive monkey populations in the USA throughout the following ten years, but no human infections were observed [1]. The virus responsible for human monkeypox is part of the Poxviridae family and the Orthopoxvirus genus, similar to the smallpox-causing variola virus. The Democratic Republic of

Received: Apr. 10, 2025.

2020 *Mathematics Subject Classification.* 47H10; 26A33; 34A08 .

Key words and phrases. monkeypox; fixed point; existence and uniqueness; Ulam-Hyers stability.

https://doi.org/10.28924/2291-8639-24-2026-2
ISSN: 2291-8639

the Congo, where most infections occurred, recorded the first human case of monkeypox in 1970. In this period, the members of the World Health Organization made an intense effort to eradicate smallpox, and in 1980, most countries discontinued the production of the Vaccinia vaccine [2, 3]. The discontinuation of Vaccinia vaccine production significantly reduced population immunity against viruses within the same family. Over the years, several countries have reported human cases of monkeypox, even though the disease was initially identified in African regions. In response to a growing number of cases in non-endemic areas, the World Health Organization (WHO) declared a global monkeypox outbreak in July 2022, following its emergence in May of the same year. Monkeypox transmission occurs through direct contact with infected animals or human-to-human interactions. The incubation period varies between 5 and 21 days, with symptoms generally appearing between 6 and 13 days. The disease typically progresses over 2 to 4 weeks, presenting symptoms such as fever, swollen lymph nodes, and a rash. Severe complications like pneumonia, encephalitis, or ocular infections may arise in rare instances. Recent data indicate that the monkeypox mortality rate ranges between 3% and 6%, with a higher risk observed in young children and individuals with pre-existing health conditions [4]. Furthermore, individuals with HIV (human immunodeficiency virus) are known to be more susceptible to severe monkeypox or even mortality in the event of infection. Bhunu et al. in [5] gave and analyzed a deterministic mathematical model of the co-infection of the HIV and monkeypox viruses.

The research conducted by Andrew et al. [6] explores complex systems dynamics through fractional calculus. The study offers fresh insights into modeling real-world phenomena by analyzing systems governed by fractional differential equations. This study critically examines the factors influencing healthcare system dynamics, addresses challenges, and proposes solutions. [7, 8]Additionally, it lays the groundwork for modeling complex systems, supporting the advancement of axiomatic methodologies in the field. The findings in [10, 25] emphasize mathematical models' crucial role in comprehending infectious disease dynamics.

Mathematical modeling has also been used to study the monkeypox virus transmission between animals and humans, [11] and between humans. [12] One study explores the monkeypox virus and its two modes of transmission-human-to-human and rodent-to-human-without relying on actual cases. The researchers formulated comprehensive mathematical results by classifying human and animal populations into three distinct groups, without relying on empirical data. The study in [3] aims to enhance the existing body of research on monkeypox by introducing a novel mathematical model that integrates real-world data to analyze disease transmission, particularly between humans and rodents. This research supports ongoing efforts in the United States to mitigate the spread of the disease.

Atangana et al. [13] developed the fractal-fractional (FF) operator, which integrates fractal and fractional concepts into a novel non-local operator for fractional differential equations. Their research investigates the existence and uniqueness of solutions. This innovative operator integrates

both fractional and fractal elements and has demonstrated its effectiveness as a valuable mathematical tool in multiple scientific disciplines, including epidemiology. For example, [14] used fractal fractional operators to investigate the co-infection of tuberculosis and HIV. Analyzed the HIV FF model during primary infection, [15]. Numerical simulations of the fractal fractional model for CC-Hemorrhagic fever were presented in [16]. For additional information and detailed analyses, see [17,18] for HIV/AIDS models and [19] for pandemic studies.

In their analysis of COVID-19, the study utilized the Atangana–Baleanu operator to examine a fractal-fractional model. The study concentrated on examining the solution's presence, distinctiveness, and Ulam-Hyers stability in the model, with adjustments to parameters like k_1 and k_2 [21,22].Gunasekar et al. analyzed the intricate dynamics of monkeypox, COVID-19, and tuberculosis using the fractal-fractional Atangana–Baleanu derivative. Their study provided valuable insights into Ulam–Hyers stability, as well as the existence and uniqueness of solutions [23,24]. Their study focused on developing a mathematical model for tuberculosis (TB) based on a specific case study from China. This study used advanced operators to look into Ulam-Hyer's stability and made a fractal-fractional order TB model using Lagrange polynomial-based numerical interpolation methods [26].

In their investigation, they applied fractional orders of the Atangana-Baleanu derivative to explore infection dynamics monkeypox. The current study looks at how different orders, such as fractal dimension and fractional order, affect the close solutions in this co-infection model. The study uses a customized numerical algorithm to analyze how two different orders influence the model's approximate solutions. Section 2 introduces the definitions of fractal fractional operators. Section 3 focuses on the model's formulation. Section 4 discusses the existence and uniqueness of the solutions. Section 5 discusses the stability of Ulam-Hyers solutions. Section 6 outlines the numerical approach utilized. Section 7 reviews the results of the numerical simulations performed in MATLAB, and section 8 concludes with the study's findings.

2. Preliminaries

In this section, we examine the fundamental concepts related to the fractal–fractional operator and introduce key definitions necessary for deriving the main results of this study. Additionally, we consider the Banach space represented as $y(t) \in C([0,1]) \to \mathbb{R}$ equipped with the norm $\|y\| = \max_{t\in[0,1]} |y(t)|$.

Definition 2.1. *Let $y \in C((a,\ b), R)$ be a fractal differentiable on $(a,\ b)$. If you have a generalized Mittag-Lefer type kernel and a fractional order of $0 < \varsigma \leq 1$ and a fractal dimension of $0 < \varepsilon \leq 1$, then this is how you define the fractal-fractional derivative of $y(t)$:*

$$ {}^{FFM}_{0}D_{t}^{\varsigma,\varepsilon}(y(t)) = \frac{\mathcal{AB}(\varsigma)}{(1-\varsigma)}\frac{d}{dt^{\varepsilon}}\int_{0}^{t} y(u)\mathcal{E}_{\varsigma}(\frac{-\varsigma}{1-\varsigma}(\Theta-u)^{\varsigma})du, $$

where $AB(\varsigma) = 1-\varsigma+\frac{\varsigma}{\gamma(\varsigma)}$ and $\frac{dy(u)}{du^{\varepsilon}} = \lim_{s\to u}\frac{y(t)-y(u)}{t^{\varepsilon}-u^{\varepsilon}}$.

Definition 2.2. *Atangana-Baleanu defines the fractal-fractional integral of $y(t)$ with a Mittag-Leffler type kernel and a fractional order $0 < \varsigma \leq 1$ as follows:*

$$ {}_0^{FFM}I_s^{\varsigma,\varepsilon}(y(t)) = \frac{\varsigma\varepsilon}{AB(\varsigma)\gamma(\varsigma)} \int_0^t u^{\varepsilon-1} y(u)(t-u)^{\varsigma-1} du + \frac{\varepsilon(1-\varsigma)t^{\varepsilon-1}}{AB(\varsigma)} y(t) \, . $$

3. Monkeypox Transmission Model

The proposed novel model examines the transmission dynamics of monkeypox between humans and rodents. In contrast to existing models, this one considers the recovery of treated humans and rodents through natural immunity. This model offers a unique perspective by including all potential interactions between these two species.

At any given time t, the total human population, denoted as N_h, comprises susceptible individuals (S_h), infected individuals (I_h), treated individuals (T_h), and those who have recovered (R_h). This relationship is expressed as:

$$ N_h = S_h + I_h + T_h + R_h. $$

Similarly, the total rodent population, represented by N_a, consists of susceptible rodents (S_a), infected rodents (I_a), and recovered rodents (R_a), defined as:

$$ N_a = S_a + I_a + R_a. $$

We then develop the model as follows [27]:

$$ \begin{aligned} \frac{dS_h}{dt} &= \pi_h - (\beta_1 I_a + \beta_2 I_h) S_h - \mu_h S_h, \\ \frac{dI_h}{dt} &= (\beta_1 I_a + \beta_2 I_h) S_h - (\gamma_h + \sigma_h + \mu_h + \delta_1) I_h, \\ \frac{dT_h}{dt} &= \sigma_h I_h - (\omega_h + \mu_h + \delta_2) T_h, \\ \frac{dR_h}{dt} &= \omega_h T_h + \gamma_h I_h - \mu_h R_h, \\ \frac{dS_a}{dt} &= \pi_a - \beta_3 I_a S_a - \mu_a S_a, \\ \frac{dI_a}{dt} &= \beta_3 I_a S_a - (\gamma_a + \mu_a) I_a, \\ \frac{dR_a}{dt} &= \gamma_a I_a - \mu_a R_a, \end{aligned} \tag{3.1} $$

We replace the first-order time derivative on the left side of the equation (3.1) with the fractal-fractional Mittag-Leffler (FFM), resulting in the FFM model. The following presents a potential formulation of the new FFM model for monkeypox:

$$ \begin{aligned} {}_0^{FFM}D^{\varsigma,\varepsilon}(S_h) &= \pi_h - (\beta_1 I_a + \beta_2 I_h) S_h - \mu_h S_h, \\ {}_0^{FFM}D^{\varsigma,\varepsilon}(I_h) &= (\beta_1 I_a + \beta_2 I_h) S_h - (\gamma_h + \sigma_h + \mu_h + \delta_1) I_h, \\ {}_0^{FFM}D^{\varsigma,\varepsilon}(T_h) &= \sigma_h I_h - (\omega_h + \mu_h + \delta_2) T_h, \end{aligned} $$

$$
\begin{aligned}
{}_0^{FFM}D^{\varsigma,\varepsilon}(R_h) &= \omega_h T_h + \gamma_h I_h - \mu_h R_h, \\
{}_0^{FFM}D^{\varsigma,\varepsilon}(S_a) &= \pi_a - \beta_3 I_a S_a - \mu_a S_a, \\
{}_0^{FFM}D^{\varsigma,\varepsilon}(I_a) &= \beta_3 I_a S_a - (\gamma_a + \mu_a) I_a, \\
{}_0^{FFM}D^{\varsigma,\varepsilon}(R_a) &= \gamma_a I_a - \mu_a R_a,
\end{aligned} \tag{3.2}
$$

The initial conditions are given by $S_h(0) = S_{h_0}$, $I_h(0) = I_{h_0}$, $T_h(0) = T_{h_0}$, $R_h(0) = R_{h_0}$, $S_a(0) = S_{a_0}$, $I_a(0) = I_{a_0}$, and $R_a(0) = R_{a_0}$. Additionally, the definitions of the parameters in the model. The model parameters provide crucial insights into virus transmission dynamics between humans and rodents. The parameter π_h represents the birth rate of humans, while π_a indicates the birth rate of rodents. The transmission rates β_1, β_2, and β_3 denote the frequency of virus transmission from infected rodents to humans, among infected humans, and between rodents, respectively. Recovery and mortality rates, such as γ_h, σ_h, ω_h, μ_h, δ_1, δ_2, γ_a, and μ_a, are essential for understanding the disease's progression and the effectiveness of treatment measures within both populations.

4. Existence and Uniqueness Results

In this section, we employ the fixed-point theorem to establish the existence and uniqueness of a solution for the proposed model. By incorporating the Atangana–Baleanu fractal-fractional integral operator into the model given in equation 3.2, along with the corresponding initial conditions, we derive the following result:

$$
\begin{aligned}
S_h(t) = S_h(0) &+ \frac{\varsigma\varepsilon}{AB(\varsigma)\gamma(\varsigma)} \int_0^t u^{\varepsilon-1}(t-u)^{\varsigma-1}[\pi_h - (\beta_1 I_a + \beta_2 I_h)S_h - \mu_h S_h]du \\
&+ \frac{\varepsilon(1-\varsigma)\Theta^{\varepsilon-1}}{AB(\varsigma)}[\pi_h - (\beta_1 I_a + \beta_2 I_h)S_h - \mu_h S_h],
\end{aligned} \tag{4.1}
$$

$$
\begin{aligned}
I_h(t) = I_h(0) &+ \frac{\varsigma\varepsilon}{AB(\varsigma)\gamma(\varsigma)} \int_0^t u^{\varepsilon-1}(t-u)^{\varsigma-1}[(\beta_1 I_a + \beta_2 I_h)S_h - (\gamma_h + \sigma_h + \mu_h + \delta_1)I_h]du \\
&+ \frac{\varepsilon(1-\varsigma)t^{\varepsilon-1}}{AB(\varsigma)}[(\beta_1 I_a + \beta_2 I_h)S_h - (\gamma_h + \sigma_h + \mu_h + \delta_1)I_h],
\end{aligned} \tag{4.2}
$$

$$
\begin{aligned}
T_h(t) = T_h(0) &+ \frac{\varsigma\varepsilon}{AB(\varsigma)\gamma(\varsigma)} \int_0^t u^{\varepsilon-1}(t-u)^{\varsigma-1}[\sigma_h I_h - (\omega_h + \mu_h + \delta_2)T_h]du \\
&+ \frac{\varepsilon(1-\varsigma)t^{\varepsilon-1}}{AB(\varsigma)}[\sigma_h I_h - (\omega_h + \mu_h + \delta_2)T_h],
\end{aligned} \tag{4.3}
$$

$$
\begin{aligned}
R_h(t) = R_h(0) &+ \frac{\varsigma\varepsilon}{AB(\varsigma)\gamma(\varsigma)} \int_0^t u^{\varepsilon-1}(t-u)^{\varsigma-1}[\omega_h T_h + \gamma_h I_h - \mu_h R_h]du \\
&+ \frac{\varepsilon(1-\varsigma)t^{\varepsilon-1}}{AB(\varsigma)}[\omega_h T_h + \gamma_h I_h - \mu_h R_h],
\end{aligned} \tag{4.4}
$$

$$S_a(t) = S_a(0) + \frac{\varsigma\varepsilon}{AB(\varsigma)\gamma(\varsigma)}\int_0^t u^{\varepsilon-1}(t-u)^{\varsigma-1}[\pi_a - \beta_3 I_a S_a - \mu_a S_a]du + \frac{\varepsilon(1-\varsigma)t^{\varepsilon-1}}{AB(\varsigma)}[\pi_a - \beta_3 I_a S_a - \mu_a S_a], \tag{4.5}$$

$$I_a(t) = I_a(0) + \frac{\varsigma\varepsilon}{AB(\varsigma)\gamma(\varsigma)}\int_0^t u^{\varepsilon-1}(t-u)^{\varsigma-1}[\beta_3 I_a S_a - (\gamma_a + \mu_a)I_a]du + \frac{\varepsilon(1-\varsigma)t^{\varepsilon-1}}{AB(\varsigma)}[\beta_3 I_a S_a - (\gamma_a + \mu_a)I_a], \tag{4.6}$$

$$R_a(t) = R_a(0) + \frac{\varsigma\varepsilon}{AB(\varsigma)\gamma(\varsigma)}\int_0^t u^{\varepsilon-1}(t-u)^{\varsigma-1}[\gamma_a I_a - \mu_a R_a]du + \frac{\varepsilon(1-\varsigma)t^{\varepsilon-1}}{AB(\varsigma)}[\gamma_a I_a - \mu_a R_a]. \tag{4.7}$$

The function K_i for $i = 1, 2, ..., 7$ or $i \in N_1^7$ will be examined

$$\begin{aligned}
K_1(t, S_h) &= \pi_h - (\beta_1 I_a + \beta_2 I_h)S_h - \mu_h S_h,\\
K_2(t, I_h) &= (\beta_1 I_a + \beta_2 I_h)S_h - (\gamma_h + \sigma_h + \mu_h + \delta_1)I_h,\\
K_3(t, T_h) &= \sigma_h I_h - (\omega_h + \mu_h + \delta_2)T_h,\\
K_4(t, R_h) &= \omega_h T_h + \gamma_h I_h - \mu_h R_h,\\
K_5(t, S_a) &= \pi_a - \beta_3 I_a S_a - \mu_a S_a,\\
K_6(t, I_a) &= \beta_3 I_a S_a - (\gamma_a + \mu_a)I_a,\\
K_7(t, R_a) &= \gamma_a I_a - \mu_a R_a.
\end{aligned}$$

($\mathcal{H}$:) In order to prove our results, we determine the following hypotheses:

For the $S_h(t), {S_h}^*(t), I_h(t), I_h^*(t), T_h(t), T_h^*(t), R_h(t), R_h^*(t), S_a(t), S_a^*(t), I_a(t), I_a^*(t), R_a(t), R_a^*(t). \in L[0,1]$ be continuous function, such that $\|S_h(t)\| \leq \mathcal{L}_1, \|I_h(t)\| \leq \mathcal{L}_2, \|T_h(t)\| \leq \mathcal{L}_3, \|R_h(t)\| \leq \mathcal{L}_4, \|S_a(\Theta)\| \leq \mathcal{L}_5, \|I_a(\Theta)\| \leq \mathcal{L}_6, \|R_a(\Theta)\| \leq \mathcal{L}_7$ for non-negative constant $\mathcal{L}_1, \mathcal{L}_2, \mathcal{L}_3, \mathcal{L}_4, \mathcal{L}_5, \mathcal{L}_6, \mathcal{L}_7 > 0$.

Theorem 4.1. *For $i \in \mathcal{N}_1^7$, if the assumption $\mathcal{H}$ is satisfied and $\chi_i < 1$ for $i \in \mathcal{N}_1^7$, then this satisfies the Lipschitz condition.*

Proof: We aim to show that $\mathcal{K}_1(t, \mathrm{S}_h)$ fulfills the Lipschitz condition. Considering $\mathrm{S}_h(t)$ and $\mathrm{S}_h^*(t)$, we derive the following:

$$\|K_1(t, S_h) - K_1(t, S_h^*)\| = \|\pi_h - (\beta_1 I_a + \beta_2 I_h(S_h - S_h^*)) - \mu_h(S_h - S_h^*)\|. \tag{4.8}$$

Considering $\eta_1 = \|\beta_1 I_a + \beta_2 I_h + \mu_h\|$, and given that I_a and I_h are bounded functions, we can derive

$$\|K_1(t,S_h)-K_1(t,S_h^*)\| \le \chi_1\|S_h-S_h^*\|, \tag{4.9}$$

Using a similar approach, the result can be derived as

$$\begin{aligned}
\|K_2(t,I_h)-K_2(t,I_h^*)\| &\le \chi_2\|I_h-I_h^*\|,\\
\|K_3(t,T_h)-K_3(t,T_h^*)\| &\le \chi_3\|T_h-T_h^*\|,\\
\|K_4(t,R_h)-K_4(t,R_h^*)\| &\le \chi_4\|R_h-R_h^*\|,\\
\|K_5(t,S_a)-K_5(t,S_a^*)\| &\le \chi_5\|S_a-S_a^*\|,\\
\|K_6(t,I_a)-K_6(t,I_a^*)\| &\le \chi_6\|I_a-I_a^*\|,\\
\|K_7(t,R_a)-K_7(t,R_a^*)\| &\le \chi_7\|R_a-R_a^*\|.
\end{aligned} \tag{4.10}$$

Consequently, for every $i \in \mathcal{N}_1^7$, all of the kernels K_j, $j \in \mathcal{N}_1^7$ satisfied the Lipschitz property with constant $\chi_i < 1$. The proof has been completed.

Now,Eqs. 4.1 to 4.7 can be rewrite as follows:

$$S_h(t) = S_h(0) + \frac{\varsigma\varepsilon}{AB(\varsigma)\gamma(\varsigma)}\int_0^t u^{\varepsilon-1}(t-u)^{\varsigma-1}K_1(u,S_h(u))du + \frac{\varepsilon(1-\varsigma)}{AB(\varsigma)}t^{\varepsilon-1}K_1(t,S_h(t)), \tag{4.11}$$

$$I_h(t) = I_h(0) + \frac{\varsigma\varepsilon}{AB(\varsigma)\gamma(\varsigma)}\int_0^t u^{\varepsilon-1}(t-u)^{\varsigma-1}K_2(u,I_h(u))du + \frac{\varepsilon(1-\varsigma)}{AB(\varsigma)}t^{\varepsilon-1}K_2(t,I_h(t)), \tag{4.12}$$

$$T_h(t) = T_h(0) + \frac{\varsigma\varepsilon}{AB(\varsigma)\gamma(\varsigma)}\int_0^t u^{\varepsilon-1}(t-u)^{\varsigma-1}K_3(u,T_h(u))du + \frac{\varepsilon(1-\varsigma)}{AB(\varsigma)}t^{\varepsilon-1}K_3(t,T_h(t)), \tag{4.13}$$

$$R_h(t) = R_h(0) + \frac{\varsigma\varepsilon}{AB(\varsigma)\gamma(\varsigma)}\int_0^t u^{\varepsilon-1}(t-u)^{\varsigma-1}K_4(u,R_h(u))du + \frac{\varepsilon(1-\varsigma)}{AB(\varsigma)}t^{\varepsilon-1}K_4(t,R_h(t)), \tag{4.14}$$

$$S_a(t) = S_a(0) + \frac{\varsigma\varepsilon}{AB(\varsigma)\gamma(\varsigma)}\int_0^t u^{\varepsilon-1}(t-u)^{\varsigma-1}K_5(u,S_a(u))du + \frac{\varepsilon(1-\varsigma)}{AB(\varsigma)}t^{\varepsilon-1}K_5(t,S_a(t)), \tag{4.15}$$

$$I_a(t) = I_a(0) + \frac{\varsigma\varepsilon}{AB(\varsigma)\gamma(\varsigma)}\int_0^t u^{\varepsilon-1}(t-u)^{\varsigma-1}K_6(u,I_a(u))du + \frac{\varepsilon(1-\varsigma)}{AB(\varsigma)}t^{\varepsilon-1}K_6(t,I_a(t)), \tag{4.16}$$

$$R_a(t) = R_a(0) + \frac{\varsigma\varepsilon}{AB(\varsigma)\gamma(\varsigma)}\int_0^t u^{\varepsilon-1}(t-u)^{\varsigma-1}K_7(u,R_a(u))du + \frac{\varepsilon(1-\varsigma)}{AB(\varsigma)}t^{\varepsilon-1}K_7(t,R_a(t)). \tag{4.17}$$

together with initial conditions are given as
$S_{h_0}(t) = S_h(0)$, $I_{h_0}(t) = I_h(0)$, $T_{h_0}(t) = T_h(0)$, $R_{h_0}(t) = R_h(0)$, $S_{a_0}(t) = S_a(0)$, $I_{a_0}(t) = I_a(0)$, *and* $R_{a_0}(t) = R_a(0)$. *The recursive formulas for Eqs.4.11 through 4.17 are now defined as follows:*

$$S_{h_n}(t) = S_h(0) + \frac{\varsigma\varepsilon}{AB(\varsigma)\gamma(\varsigma)}\int_0^t u^{\varepsilon-1}(t-u)^{\varsigma-1}K_1(u,S_{h_{n-1}}(u))du + \frac{\varepsilon(1-\varsigma)}{AB(\varsigma)}t^{\varepsilon-1}K_1(t,S_{h_{n-1}}(t)),$$

$$I_{h_n}(t) = I_{h(0)} + \frac{\varsigma\varepsilon}{AB(\varsigma)\gamma(\varsigma)}\int_0^t u^{\varepsilon-1}(t-u)^{\varsigma-1}K_2(u, I_{h_{n-1}}(u))du + \frac{\varepsilon(1-\varsigma)}{AB(\varsigma)}t^{\varepsilon-1}K_2(t, I_{h_{n-1}}(t)),$$

$$T_{h_n(t)} = T_{h(0)} + \frac{\varsigma\varepsilon}{AB(\varsigma)\gamma(\varsigma)}\int_0^{\Theta} u^{\varepsilon-1}(t-u)^{\varsigma-1}K_3(u, T_{h_{n-1}}(u))du + \frac{\varepsilon(1-\varsigma)}{AB(\varsigma)}t^{\varepsilon-1}K_3(t, T_{h_{n-1}}(t)),$$

$$R_{h_n(t)} = R_{h(0)} + \frac{\varsigma\varepsilon}{AB(\varsigma)\gamma(\varsigma)}\int_0^t u^{\varepsilon-1}(t-u)^{\varsigma-1}K_4(u, R_{h_{n-1}}(u))du + \frac{\varepsilon(1-\varsigma)}{AB(\varsigma)}t^{\varepsilon-1}K_4(t, R_{h_{n-1}}(t)),$$

$$S_{a_n(t)} = S_{a(0)} + \frac{\varsigma\varepsilon}{AB(\varsigma)\gamma(\varsigma)}\int_0^t u^{\varepsilon-1}(t-u)^{\varsigma-1}K_5(u, S_{a_{n-1}}(u))du + \frac{\varepsilon(1-\varsigma)}{AB(\varsigma)}t^{\varepsilon-1}K_5(t, S_{a_{n-1}}(\Theta)),$$

$$I_{a_n(t)} = I_{a(0)} + \frac{\varsigma\varepsilon}{AB(\varsigma)\gamma(\varsigma)}\int_0^t u^{\varepsilon-1}(t-u)^{\varsigma-1}K_6(u, I_{a_{n-1}}(u))du + \frac{\varepsilon(1-\varsigma)}{AB(\varsigma)}t^{\varepsilon-1}K_6(t, I_{a_{n-1}}(t)),$$

$$R_{a_n(t)} = R_{a(0)} + \frac{\varsigma\varepsilon}{AB(\varsigma)\gamma(\varsigma)}\int_0^t u^{\varepsilon-1}(t-u)^{\varsigma-1}K_7(u, R_{a_{n-1}}(u))du + \frac{\varepsilon(1-\varsigma)}{AB(\varsigma)}t^{\varepsilon-1}K_7(t, R_{a_{n-1}}(t)).$$

Theorem 4.2. *If the following conditions are satisfied, the model 3.2 has a solution:*

$$\triangle = max\delta_i < 1, i \in N_1^7.$$

Proof: The functions are defined as follows:

$$\begin{aligned}
\Xi_{1_n}(t) &= S_{h_{n+1}}(t) - S_h(t),\\
\Xi_{2_n}(t) &= I_{h_{n+1}}(t) - I_h(t),\\
\Xi_{3_n}(t) &= T_{h_{n+1}}(t) - T_h(t),\\
\Xi_{4_n}(t) &= R_{h_{n+1}}(t) - R_h(t),\\
\Xi_{5_n}(t) &= S_{a_{n+1}}(t) - S_a(t),\\
\Xi_{6_n}(t) &= I_{a_{n+1}}(t) - I_a(t),\\
\Xi_{7_n}(t) &= R_{a_{n+1}}(t) - R_a(t).
\end{aligned} \tag{4.18}$$

Then, we find that

$$\begin{aligned}
\|\Xi_{1_n}(t)\| &= \frac{\varsigma\varepsilon}{AB(\varsigma)\gamma(\varsigma)}\int_0^t u^{\varepsilon-1}(t-u)^{\varsigma-1}\|K_1(u, S_{h_n}(u)) - K_1(u, S_{h_n}(u))\|du\\
&\quad + \frac{\varepsilon(1-\varsigma)t^{\varepsilon-1}}{AB(\varsigma)}\|K_1(t, S_{h_{n_1}}(t)) - K_1(t, S_h(t))\|,\\
&\leq \left[\frac{\varsigma\varepsilon\gamma(\varepsilon)}{AB(\varsigma)\gamma(\varsigma+\varepsilon)} + \frac{\varepsilon(1-\varsigma)}{AB(\varsigma)}\right]\delta_1\|S_{h_n} - S_h\|\\
&\leq \left[\frac{\varsigma\varepsilon\gamma(\varepsilon)}{AB(\varsigma)\gamma(\varsigma+\varepsilon)} + \frac{\varepsilon(1-\varsigma)}{AB(\varsigma)}\right]^n\delta_1^n\|S_{h_1} - S_h\|.
\end{aligned}$$

Similarly, we have

$$\|\Xi_{2_n}(t)\| \leq \left[\frac{\varsigma\varepsilon\gamma(\varepsilon)}{AB(\varsigma)\gamma(\varsigma+\varepsilon)} + \frac{\varepsilon(1-\varsigma)}{AB(\varsigma)}\right]^n\delta_2^n\|I_{h_1} - I_h\|,$$

$$\|\Xi_{3_n}(t)\| \leq \left[\frac{\varsigma\varepsilon\gamma(\varepsilon)}{AB(\varsigma)\gamma(\varsigma+\varepsilon)} + \frac{\varepsilon(1-\varsigma)}{AB(\varsigma)}\right]^n\delta_3^n\|T_{h_1} - T_h\|,$$

$$\|\Xi_{4_n}(t)\| \leq \left[\frac{\varsigma\varepsilon\gamma(\varepsilon)}{AB(\varsigma)\gamma(\varsigma+\varepsilon)} + \frac{\varepsilon(1-\varsigma)}{AB(\varsigma)}\right]^n \delta_4^n \|R_{h_1} - R_a\|,$$

$$\|\Xi_{5_n}(t)\| \leq \left[\frac{\varsigma\varepsilon\gamma(\varepsilon)}{AB(\varsigma)\gamma(\varsigma+\varepsilon)} + \frac{\varepsilon(1-\varsigma)}{AB(\varsigma)}\right]^n \delta_5^n \|S_{a_1} - S_a\|,$$

$$\|\Xi_{6_n}(\Theta)\| \leq \left[\frac{\varsigma\varepsilon\gamma(\varepsilon)}{AB(\varsigma)\gamma(\varsigma+\varepsilon)} + \frac{\varepsilon(1-\varsigma)}{AB(\varsigma)}\right]^n \delta_6^n \|I_{a_1} - I_a\|,$$

$$\|\Xi_{7_n}(\Theta)\| \leq \left[\frac{\varsigma\varepsilon\gamma(\varepsilon)}{AB(\varsigma)\gamma(\varsigma+\varepsilon)} + \frac{\varepsilon(1-\varsigma)}{AB(\varsigma)}\right]^n \delta_7^n \|R_{a_1} - R_a\|.$$

Therefore, the proof is complete when $n \to \infty$ and $\Xi(t)_{i_n} \to 0$ for $i \in N_1^7$ for $\delta_i < 1, (i = 1, 2, ..., 7)$. This is based on the nine functions mentioned above.

Theorem 4.3. *Assumption H indicates that the model 3.2 has a unique solution if*

$$\left[\frac{\varsigma\varepsilon\gamma(\varepsilon)}{AB(\varsigma)\gamma(\varsigma+\varepsilon)} + \frac{\varepsilon(1-\varsigma)}{AB(\varsigma)}\right]\delta_i \leq 1, i = 1, 2, ..., 7.$$

Proof

We assume that another existing solution $(S_h^*(t), I_h^*(t), T_h^*(t), R_h^*(t), S_a^*(t), I_a^*(t), R_a^*(t).)$ with initial values,such that

$$S^*(t) = S^*(0) + \frac{\varsigma\varepsilon}{AB(\varsigma)\gamma(\varsigma)} \int_0^t u^{\varepsilon-1}(t-u)^{\varsigma-1} K_1(u, S^*(u))du + \frac{\varepsilon(1-\varsigma)t^{\varepsilon-1}}{AB(\varsigma)} K_1(t, S(t)).$$

Now, we write

$$\|S_h - {S_h}^*\| = \frac{\varsigma\varepsilon}{AB(\varsigma)\gamma(\varsigma)} \int_0^t u^{\varepsilon-1}(t-u)^{\varsigma-1} \|K_1(u, S_h(u)) - K_1(u, {S_h}^*(u))\|du$$

$$+ \frac{\varepsilon(1-\varsigma)t^{\varepsilon-1}}{AB(\varsigma)} \|K_1(u, S_h(u)) - K_1(u, {S_h}^*(u))\|$$

$$\leq \frac{\varsigma\varepsilon}{AB(\varsigma)\gamma(\varsigma)} \int_0^t u^{\varepsilon-1}(t-u)^{\varsigma-1} \Phi_1 \|S_h - S_h^*\| + \frac{\varepsilon(1-\varsigma)\Theta^{\varepsilon-1}}{AB(\varsigma)} \Phi_1 \|S_h - S_h^*\|$$

$$\leq \left[\frac{\varsigma\varepsilon}{AB(\varsigma)\gamma(\varsigma+\varepsilon)} + \frac{\varepsilon(1-\varsigma)}{AB(\varsigma)}\right]\Phi_1 \|S_h - {S_h}^*\|$$

and so

$$\left[1 - \left[\frac{\varsigma\varepsilon}{AB(\varsigma)\gamma(\varsigma+\varepsilon)} + \frac{\varepsilon(1-\varsigma)}{AB(\varsigma)}\right]\Phi_1\right]\|S_h - {S_h}^*\| \leq 0. \tag{4.19}$$

The inequality in equation (3.19) is valid when $\|S_h - {S_h}^*\| = 0$, which leads to the conclusion that $S_h(t) = {S_h}^*(t)$. This establishes the uniqueness of the solution. A similar method is applied to I_h, T_h, R_h, S_a, I_a, and R_a, confirming the uniqueness of the solutions for these variables as well. Therefore, the model described by equation 3.2 has a unique solution.

5. Ulam-Hyers Stability

The Ulam-Hyers stability of the model shown in equation 3.2 is established in this section. To do so, we will introduce the necessary definition for this purpose.

Definition 5.1. *Ulam-Hyers stability for the model 3.2 is satisfied if $\zeta_i > 0, i \in n_1^7$. For every $\ell_i > 0, i \in n_1^7$, if*

$$\begin{aligned}
&|{}_0^{FFM}D^{\varsigma,\varepsilon}S_h(t) - K_1(t,S_h)| \leq \ell_1,\\
&|{}_0^{FFM}D^{\varsigma,\varepsilon}I_h(t) - K_2(t,I_h)| \leq \ell_2,\\
&|{}_0^{FFM}D^{\varsigma,\varepsilon}T_h(t) - K_3(t,T_h)| \leq \ell_3,\\
&|{}_0^{FFM}D^{\varsigma,\varepsilon}R_h(t) - K_4(t,R_h)| \leq \ell_4,\\
&|{}_0^{FFM}D^{\varsigma,\varepsilon}S_a(t) - K_5(t,S_a)| \leq \ell_5,\\
&|{}_0^{FFM}D^{\varsigma,\varepsilon}I_a(t) - K_6(t,I_a)| \leq \ell_6,\\
&|{}_0^{FFM}D^{\varsigma,\varepsilon}R_a(t) - K_7(t,R_a)| \leq \ell_7.
\end{aligned} \tag{5.1}$$

Additionally, the monkeypox model 3.2 has a solution. $S_h^*(t), I_h^*(t), T_h^*(t), R_h^*(t), S_a^*(t), I_a^*(t)$ and $R^*(t)$, that satisfying the given model,
such that

$$\|S_h - S_h^*\| \leq \zeta_1\ell_1, \|I_h - I_h^*\| \leq \zeta_2\ell_2, \|T_h - T_h^*\| \leq \zeta_3\ell_3, \|R_h - R_h^*\| \leq \zeta_4\ell_4, \|S_a - S_a^*\| \leq \zeta_5\ell_5,$$

$$\|I_a - I_a^*\| \leq \zeta_6\ell_6, \|R_a - R_a^*\| \leq \zeta_7\ell_7.$$

Remark 5.1. *If there is a continuous function h_1, then let us consider that the function S^* is a solution to the first inequality (5.22).*
(a) $|h_1(t)| < \ell_1$, and
(b) ${}_0^{FFM}D^{\varsigma,\varepsilon}S_h(t) - K_1(t,S_h) + h_1(t)$.
Similarly, by determining h_i for $i \in N_2^7$, one can indicate such a definition for every solution to inequalities (5.22).

Theorem 5.1. *The Ulam-Hyers stable model 3.2 is under the assumption H.*
Proof. *Let $\ell_1 > 0$ and S be an arbitrary function such that*

$${}_0^{FFM}D^{\varsigma,\varepsilon}S_h(t) - K_1(t,S_h)| \leq \ell_1$$

In view of Remark1, we have a function $h_1$with $|h_1(t)| < \ell_1$ satisfies

$${}_0^{FFM}D^{\varsigma,\varepsilon}S_h(t) - K_1(t,S_h) + h_1(t)$$

Consequently,

$$\begin{aligned}
S_h(t) = S_h(0) &+ \frac{\varsigma\varepsilon}{AB(\varsigma)\gamma(\varsigma)}\int_0^{\Theta} u^{\varepsilon-1}(t-u)^{\varsigma-1}K_1(u,S_h(u))du + \frac{\varepsilon(1-\varsigma)}{AB(\varsigma)}t^{\varepsilon-1}K_1(t,S_h(t))\\
&+\frac{\varsigma\varepsilon}{AB(\varsigma)\gamma(\varsigma)}\int_0^{t} u^{\varepsilon-1}(t-u)^{\varsigma-1}h_1(u))du + \frac{\varepsilon(1-\varsigma)}{AB(\varsigma)}t^{\varepsilon-1}h_1(t))
\end{aligned}$$

Given the model and its unique solution S_h^*,

$$S_h^*(t) = S_h^*(0) + \frac{\varsigma\varepsilon}{AB(\varsigma)\gamma(\varsigma)}\int_0^t u^{\varepsilon-1}(t-u)^{\varsigma-1}K_1(u,S_h(u))du + \frac{\varepsilon(1-\varsigma)}{AB(\varsigma)}t^{\varepsilon-1}K_1(t,S_h(t))$$

Hence,

$$\begin{aligned}|S_h(t) - S_h^*(t)| \leq \frac{\varsigma\varepsilon}{AB(\varsigma)\Gamma(\varsigma)}\int_0^t u^{\varepsilon-1}(t-u)^{\varsigma-1}|K_1(u,S_h(u)) - K_1(u,S_h^*(u))|du,\\ + \frac{\varepsilon(1-\varsigma)}{AB(\varsigma)}t^{\varepsilon-1}|K_1(u,S_h(u)) - K_1(u,S_h^*(u))|\\ + \frac{\varsigma\varepsilon}{AB(\varsigma)\gamma(\varsigma)}\int_0^t u^{\varepsilon-1}(t-u)^{\varsigma-1}|h_1(u)|du + \frac{\varepsilon(1-\varsigma)}{AB(\varsigma)}t^{\varepsilon-1}|h_1(t)|,\\ \leq \left[\frac{\varsigma\varepsilon\gamma(\varepsilon)}{AB(\varsigma)\gamma(\varsigma+\varepsilon)} + \frac{\varepsilon(1-\varsigma)}{AB(\varsigma)}\right]\delta_1|S_h - S_h^*| + \left[\frac{\varsigma\varepsilon\gamma(\varepsilon)}{AB(\varsigma)\gamma(\varsigma+\varepsilon)} + \frac{\varepsilon(1-\varsigma)}{AB(\varsigma)}\right]\ell_1,\\ \|S - S^*\| \leq \frac{\left[\frac{\varsigma\varepsilon\gamma(\varepsilon)}{AB(\varsigma)\gamma(\varsigma+\varepsilon)} + \frac{\varepsilon(1-\varsigma)}{AB(\varsigma)}\right]\ell_1}{1 - \left[\frac{\varsigma\varepsilon\gamma(\varepsilon)}{AB(\varsigma)\gamma(\varsigma+\varepsilon)} + \frac{\varepsilon(1-\varsigma)}{AB(\varsigma)}\right]\delta_1}.\end{aligned}$$

Then

$$\|S_h - S_h^*\| \leq \zeta_1\ell_1.$$

If, we take

$$\zeta_1 = \frac{\left[\frac{\varsigma\varepsilon\gamma(\varepsilon)}{AB(\varsigma)\gamma(\varsigma+\varepsilon)} + \frac{\varepsilon(1-\varsigma)}{AB(\varsigma)}\right]}{1 - \left[\frac{\varsigma\varepsilon\gamma(\varepsilon)}{AB(\varsigma)\gamma(\varsigma+\varepsilon)} + \frac{\varepsilon(1-\varsigma)}{AB(\varsigma)}\right]\delta_1}.$$

Now,applying a similarly

$$\begin{aligned}\|I_h - I_h^*\| &\leq \zeta_2\ell_2.\\ \|T_h - T_h^*\| &\leq \zeta_3\ell_3.\\ \|R_h - R_h^*\| &\leq \zeta_4\ell_4.\\ \|S_a - S_a^*\| &\leq \zeta_5\ell_5.\\ \|I_a - I_a^*\| &\leq \zeta_6\ell_6.\\ \|R_a - R_a^*\| &\leq \zeta_7\ell_7.\end{aligned}$$

Thus, we deduce Ulam-Hyers stability for the fractal-fractional model 3.2. This ends the proof.

6. Numerical Scheme

In this section, we introduce the numerical scheme associated with the model described in equation 3.2. Specifically, we examine the structure and formulation of the Atangana–Baleanu fractional operator equation:

$${}_0^{FFM}D^{\varsigma,\varepsilon}\chi(t) = \varepsilon t^{\varepsilon-1}\delta(t,\chi(t)).$$

We obtain the following result by using a generalized Mittag-Leffler type kernel in conjunction with the fractal-fractional integral operator:

$$\chi(t) = \chi(0) + \frac{\varepsilon(1-\varsigma)}{AB(\varsigma)} t_n^{\varepsilon-1} \delta(t, \chi(\Theta)) + \frac{\varsigma\varepsilon}{AB(\varsigma)\gamma\varsigma} \int_0^t u^{\varepsilon-1}(t-u)^{\varsigma-1} \delta(u, \chi(u)) du.$$

Putting t by t_{n+1} we find

$$\chi(t) = \chi(0) + \frac{\varepsilon(1-\varsigma)}{AB(\varsigma)} t_n^{\varepsilon-1} \delta(t_n, \chi(t_n)) + \frac{\varsigma\varepsilon}{AB(\varsigma)\gamma\varsigma} \int_0^{t_{n+1}} u^{\varepsilon-1}(t_{n+1}-u)^{\varsigma-1} \delta(u, \chi(u)) du. \tag{6.1}$$

By applying the Lagrange polynomial approach, we derive the following result:

$$\begin{aligned}
\delta(y, \chi(t)) &= \frac{(y - t_{\nu_0-1}) v(t_{\nu_0}, \chi(\Theta_{\nu_0}))}{t_{\nu_0} - t_{\nu_0-1}} - \frac{(y - t_{\nu_0}) v(t_{\nu_0-1}, \chi t_{\nu_0-1})}{t_{\nu_0} - t_{\nu_0-1}} \\
&= \frac{\delta(t_{\nu_0}, \chi(t_{\nu_0}))(y - t_{\nu_0-1})}{t_{\nu_0} - t_{\nu_0-1}} - \frac{\delta(t_{\nu_0-1}, \chi(t_{\nu_0-1}))(y - t_{\nu_0})}{t_{\nu_0} - t_{\nu_0-1}} \\
&= \frac{\delta(t_{\nu_0}, \chi(t_{\nu_0}))(y - t_{\nu_0-1})}{h} - \frac{\delta(t_{\nu_0-1}, \chi(t_{\nu_0-1}))(y - t_{\nu_0})}{h}
\end{aligned}$$

using the Lagrange polynomial for (5.21),we get

$$\begin{aligned}
\chi^{n+1} =& \chi(0) + \frac{(1-\varsigma)}{AB(\varsigma)} \delta(t_n, \chi(t_n)) \\
&+ \frac{\varsigma\varepsilon}{AB(\varsigma)\gamma(\varsigma)} \sum_{\nu_0=1}^{n} \Big[\frac{\delta(t_{\nu_0}, \chi(t_{\nu_0}))}{h} \int_{t_{\nu_0}}^{t_{\nu_0+1}} (u - t_{\nu_0-1})(t_{n+1} - u)^{\varsigma-1} du \\
&- \frac{\delta(t_{\nu_0} - 1, \chi(t_{\nu_0} - 1))}{h} \int_{t_{\nu_0}}^{t_{\nu_{n+1}}} (u - t_{\nu_0})(t_{n+1} - u)^{\varsigma-1} du \Big]
\end{aligned}$$

solving the integral equation above, we get

$$\begin{aligned}
\chi^{n+1} =& \chi(0) + \frac{(1-\varsigma)}{AB(\varsigma)} \delta(t_n, \chi(t_n)) \\
&+ \frac{\varsigma h^{\varsigma}}{AB(\varsigma)\gamma(\varsigma+2)} \sum_{\nu_0=1}^{n} \Big[\delta(t_{\nu_0}, \chi(t_{\nu_0})) \Big((n+1-\nu_0)^{\varsigma}(n-\nu_0+2+\varsigma) \\
&- (n-\nu_0)^{\varsigma}(n+2-\nu_0+2\varsigma) \Big) \\
&- \delta(t_{\nu_0-1}, \chi_{\nu_0-1}) \Big((n+1-\nu_0)^{\varsigma+1} - (n-\nu_0+1+\varsigma)(n-\nu_0)^{\varsigma} \Big)
\end{aligned}$$

using $\delta(t, \chi(t))$, we obtain

$$\begin{aligned}
\chi^{n+1} =& \chi(0) + \varepsilon t_n^{\varepsilon-1} \frac{1-\varsigma}{AB(\varsigma)} Q(t_n, \chi(t_n)) \\
&+ \frac{\varepsilon h^{\varsigma}}{AB(\varsigma)\gamma(\varsigma+2)} \sum_{\nu_0=1}^{n} \Big[t_{\nu_0}^{\varepsilon-1} \mathfrak{R}(t_{\nu_0}, \chi(t_{\nu_0})) \Big((n+1-\nu_0)^{\varsigma}(n-\nu_0+2+\varsigma) \\
&- (n-\nu_0)^{\varsigma}(n+2-\nu_0+2\varsigma) \Big) \\
&-_{\nu_0}^{\varepsilon-1} \mathfrak{R}(t_{\nu_0-1}, \chi t_{\nu_0-1}) \Big((n+1-\nu_0)^{\varsigma+1} - (n-\nu_0+1+\varsigma)(n-\nu_0)^{\varsigma} \Big) \Big].
\end{aligned}$$

Therefore, by presuming

$\aleph_1(n,\nu_0) := (n+1-\nu_0)^{\varsigma}(n-\nu_0+2+\varsigma) - (n-\nu_0)^{\varsigma}(n+2-\nu_0+2\varsigma)$

$\aleph_2(n,\nu_0) := (n+1-\nu_0)^{\varsigma+1} - (n-\nu_0+1+\varsigma)(n-\nu_0)^{\varsigma}$

Hence, the numerical scheme for 6.1 is obtained as

$$S_h(t_{n+1}) = S_h(0) + \varepsilon t_n^{\varepsilon-1}\frac{1-\varsigma}{AB(\varsigma)}K_1(t_n, S_h(t_n)) + \frac{\varepsilon h^{\varsigma}}{AB(\varsigma)\gamma(\varsigma+2)} \times \sum_{\nu_0=1}^{n}\left[t_{\nu_0}^{\varepsilon-1}K_1(t_{\nu_0}, S(t_{\nu_0}))\aleph_1(n,\nu_0) - t_{\nu_0-1}^{\varepsilon-1}K_1(t_{\nu_0-1}, S_h(t_{\nu_0-1}))\aleph_2(n,\nu_0)\right], \tag{6.2}$$

$$I_h(t_{n+1}) = I_h(0) + \varepsilon t_n^{\varepsilon-1}\frac{1-\varsigma}{AB(\varsigma)}K_2(t_n, I_h(t_n)) + \frac{\varepsilon h^{\varsigma}}{AB(\varsigma)\gamma(\varsigma+2)} \times \sum_{\nu_0=1}^{n}\left[t_{\nu_0}^{\varepsilon-1}K_2(t_{\nu_0}, I_h(t_{\nu_0}))\aleph_1(n,\nu_0) - t_{\nu_0-1}^{\varepsilon-1}K_2(t_{\nu_0-1}, I_h(t_{\nu_0-1}))\aleph_2(n,\nu_0)\right], \tag{6.3}$$

$$T_h(t_{n+1}) = T_h(0) + \varepsilon t_n^{\varepsilon-1}\frac{1-\varsigma}{AB(\varsigma)}K_3(t_n, T_h(t_n)) + \frac{\varepsilon h^{\varsigma}}{AB(\varsigma)\gamma(\varsigma+2)} \times \sum_{\nu_0=1}^{n}\left[t_{\nu_0}^{\varepsilon-1}K_3(t_{\nu_0}, T_h(t_{\nu_0}))\aleph_1(n,\nu_0) - t_{\nu_0-1}^{\varepsilon-1}K_3 t_{\nu_0-1}, T_h(t_{\nu_0-1}))\aleph_2(n,\nu_0)\right], \tag{6.4}$$

$$R_h(t_{n+1}) = R_h(0) + \varepsilon t_n^{\varepsilon-1}\frac{1-\varsigma}{AB(\varsigma)}K_4(t_n, R_h(t_n)) + \frac{\varepsilon h^{\varsigma}}{AB(\varsigma)\gamma(\varsigma+2)} \times \sum_{\nu_0=1}^{n}\left[t_{\nu_0}^{\varepsilon-1}K_4(t_{\nu_0}, R_h(t_{\nu_0}))\aleph_1(n,\nu_0) - t_{\nu_0-1}^{\varepsilon-1}K_4(t_{\nu_0-1}, R_h(t_{\nu_0-1}))\aleph_2(n,\nu_0)\right], \tag{6.5}$$

$$S_a(t_{n+1}) = S_a(0) + \varepsilon t_n^{\varepsilon-1}\frac{1-\varsigma}{AB(\varsigma)}K_5(t_n, S_a(t_n)) + \frac{\varepsilon h^{\varsigma}}{AB(\varsigma)\gamma(\varsigma+2)} \times \sum_{\nu_0=1}^{n}\left[t_{\nu_0}^{\varepsilon-1}K_5(t_{\nu_0}, S_a(t_{\nu_0}))\aleph_1(n,\nu_0) - t_{\nu_0-1}^{\varepsilon-1}K_5(t_{\nu_0-1}, S_a(t_{\nu_0-1}))\aleph_2(n,\nu_0)\right], \tag{6.6}$$

$$I_a(t_{n+1}) = I_a(0) + \varepsilon t_n^{\varepsilon-1}\frac{1-\varsigma}{AB(\varsigma)}K_6(t_n, I_a(t_n)) + \frac{\varepsilon h^{\varsigma}}{AB(\varsigma)\gamma(\varsigma+2)} \times \sum_{\nu_0=1}^{n}\left[t_{\nu_0}^{\varepsilon-1}K_6(t_{\nu_0}, I_a(t_{\nu_0}))\aleph_1(n,\nu_0) - t_{\nu_0-1}^{\varepsilon-1}K_6(t_{\nu_0-1}, I_a(t_{\nu_0-1}))\aleph_2(n,\nu_0)\right], \tag{6.7}$$

$$R_a(t_{n+1}) = R_a(0) + \varepsilon t_n^{\varepsilon-1}\frac{1-\varsigma}{AB(\varsigma)}K_7(t_n, R_a(t_n)) + \frac{\varepsilon h^{\varsigma}}{AB(\varsigma)\gamma(\varsigma+2)} \times \sum_{\nu_0=1}^{n}\left[t_{\nu_0}^{\varepsilon-1}K_7(t_{\nu_0}, R_a(t_{\nu_0}))\aleph_1(n,\nu_0) - t_{\nu_0-1}^{\varepsilon-1}K_7(t_{\nu_0-1}, R_a(t_{\nu_0-1}))\aleph_2(n,\nu_0)\right]. \tag{6.8}$$

7. Fractal-Fractional Numerical Simulations.

In this section, we present the numerical results obtained using the Adams–Bashforth method for the solutions (6.24)–(6.30) to validate the accuracy of our study. The computations are performed while considering both fractal and fractional orders. Initially, iterations are carried out by varying the fractal order while keeping the fractional order fixed, followed by iterations where the fractional order varies while maintaining a constant fractal order. This approach enables an in-depth analysis of the system's behavior under different conditions. The numerical solution is obtained using the FDE12 function in MATLAB 2018, allowing us to evaluate the impact of different treatment strategies.

We took various parameter values from references along with other assumed parameters. Parameter values from [27] were also employed, including $\pi_h = 0.029$, $\pi_a = 0.80$, $\beta_1 = 0.00025$, $\beta_2 = 0.0006$, $\beta_3 = 0.035$, $\mu_h = 0.02$, $\mu_a = 0.10$, $\gamma_h = \frac{1}{21}$, $\gamma_a = \frac{1}{10}$, $\sigma_h = 0.00025$, $\delta_1 = 0.2$, $\delta_2 = 0.4$, $\omega_h = 0.004$, and the fractional-fractal order $\varsigma, \varepsilon \in [0, 1]$.

This study analyzes the transmission dynamics of Monkeypox by examining different fractional and fractal values to evaluate the impact of the fractal-fractional derivative model on disease progression. Additionally, the research seeks to identify key parameters that play a crucial role in influencing the spread of Monkeypox. A graphical analysis is performed by altering specific parameter values to observe their effects on various compartments and overall disease dynamics. The findings from this analysis can contribute to developing effective control measures for disease management.

The graphical results presented in Fig. 5 were generated using the method. These figures illustrate the dynamics of the susceptible population while also showcasing the characteristics of the infected, treated, recovered, and control groups. The control measures effectively reduce the number of infected individuals and improve treatment and recovery rates. We investigate various values of the human-to-human contact rate in Fig. 5 to assess its impact on the dynamics of the disease, focusing on the susceptible, infected, treated, and recovered human compartments. As depicted in Figures 1(a)–1(d), an increase in the human-to-human contact rate toward unity leads to more individuals becoming infected with monkeypox, resulting in a corresponding rise in treatment rates. This increase in susceptibility subsequently drives up both infection and treatment rates. Additionally, Figures 9 illustrate the dynamics of the susceptible, infected, and recovery animal populations. while simulation for fractal has been done for the time 30 days

The graphical results shown in Fig. 14 were generated using the specified method. These figures depict the dynamics of the susceptible population and highlight the characteristics of the infected, treated, recovered, and control groups. The implemented control measures successfully reduce the number of infected individuals while enhancing treatment and recovery rates.

We explore various values of the human-to-human contact rate in Fig. 14 to evaluate its influence on the disease dynamics, concentrating on the susceptible, infected, treated, and recovered human compartments. As illustrated in Figures 3(a)–3(d), increasing the human-to-human contact rate

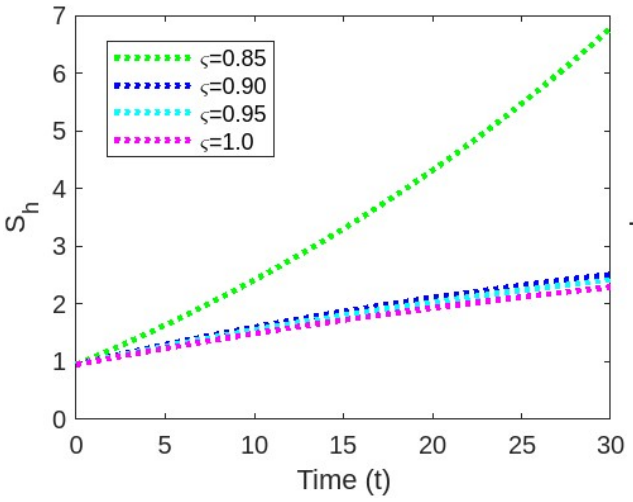

FIGURE 1. *
(a) Fractal Susceptible Population.

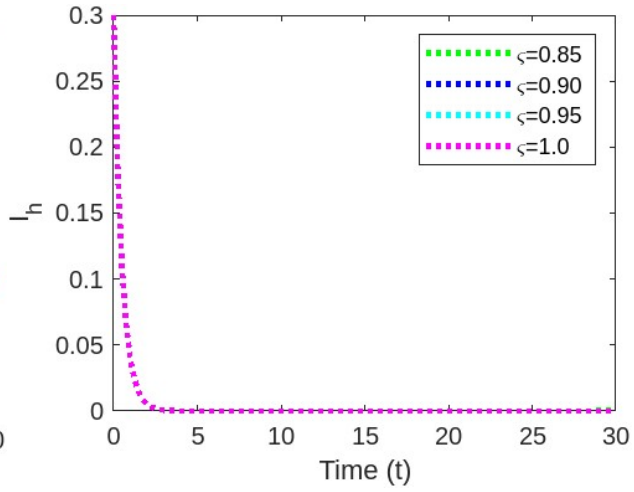

FIGURE 2. *
(b) Fractal Infected Population.

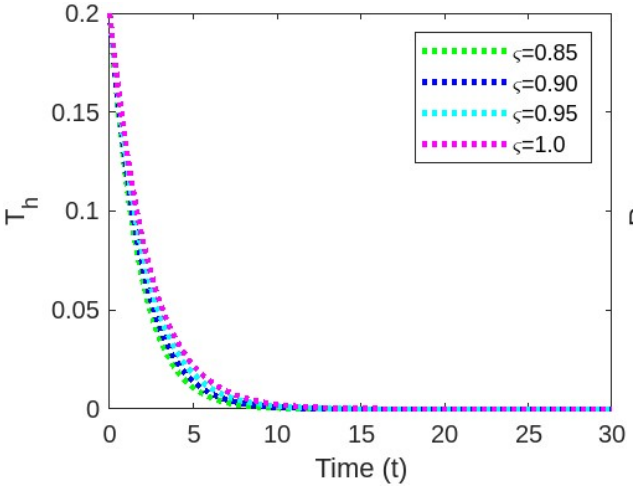

FIGURE 3. *
(c) Fractal Treatment Population.

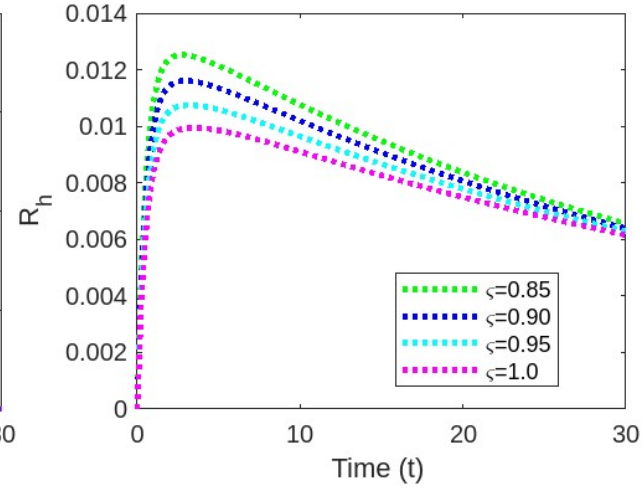

FIGURE 4. *
(d) Fractal Recovered Population.

FIGURE 5. Combined Fractal Population Graphs.

toward unity results in more individuals becoming infected with monkeypox, leading to a corresponding rise in treatment rates. This heightened susceptibility further contributes to increased infection and treatment rates. Additionally, Figures 18 present the dynamics of the susceptible, infected, and recovered animal populations. The simulation for the fractional model has been conducted over 60 days.

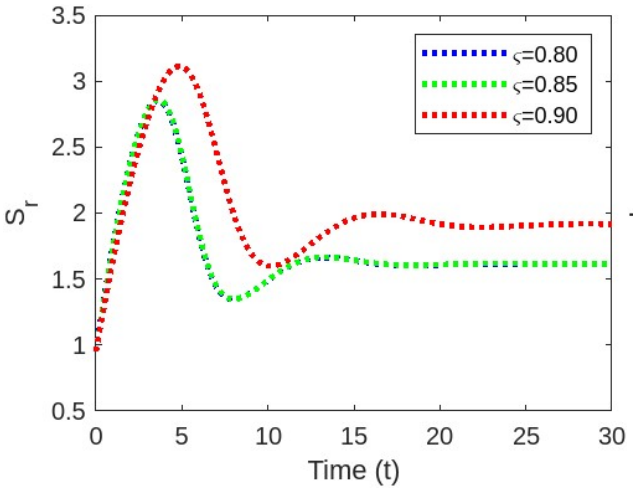

FIGURE 6. *
(a) Fractal Susceptible Rodents.

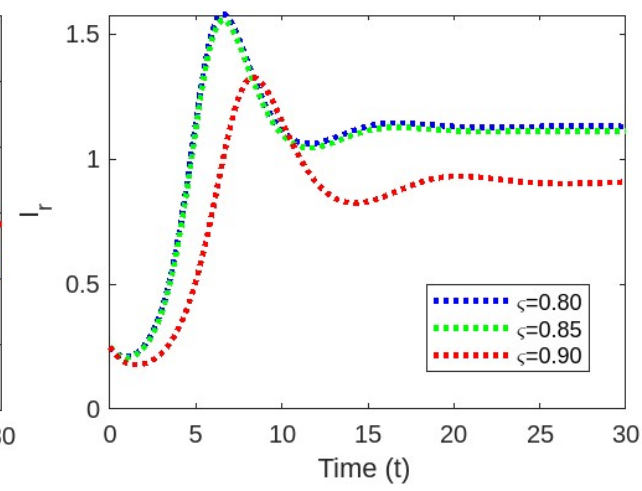

FIGURE 7. *
(b) Fractal Infected Rodents.

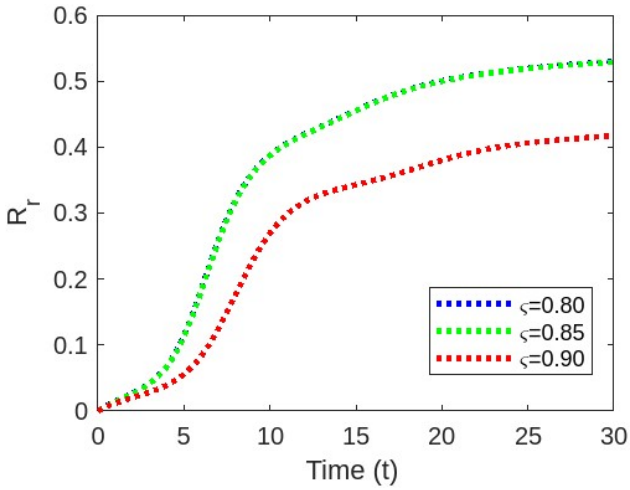

FIGURE 8. *
(c) Fractal Recovered Rodents.

FIGURE 9. Combined Fractal Rodent Populations.

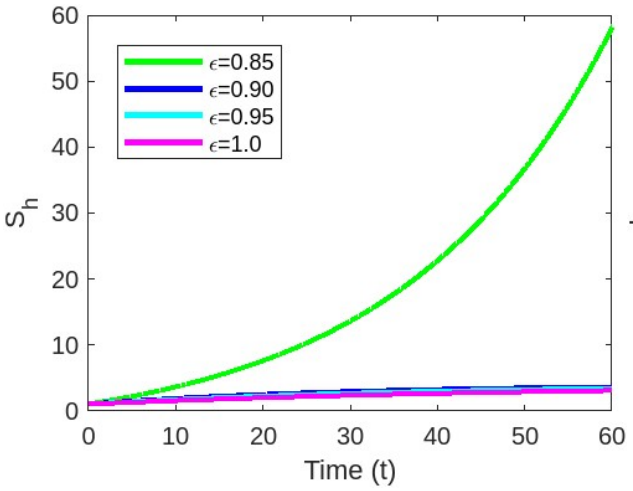

FIGURE 10. *

(a) Fractional Susceptible Population.

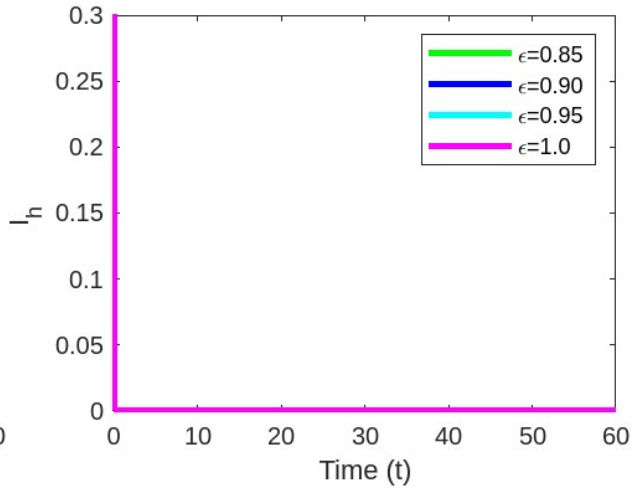

FIGURE 11. *

(b) Fractional Infected Population.

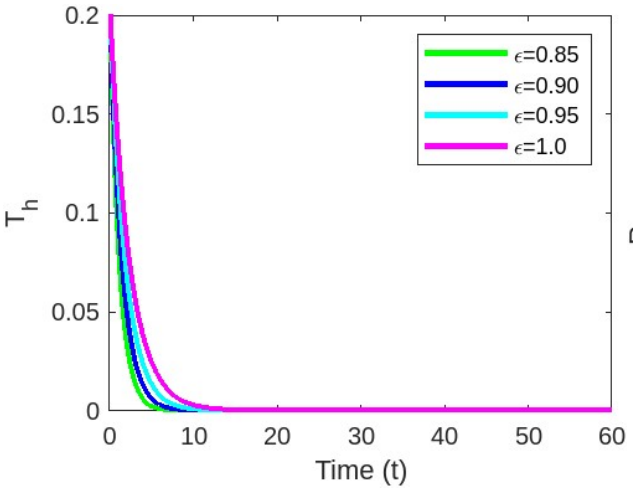

FIGURE 12. *

(c) Fractional Treatment Population.

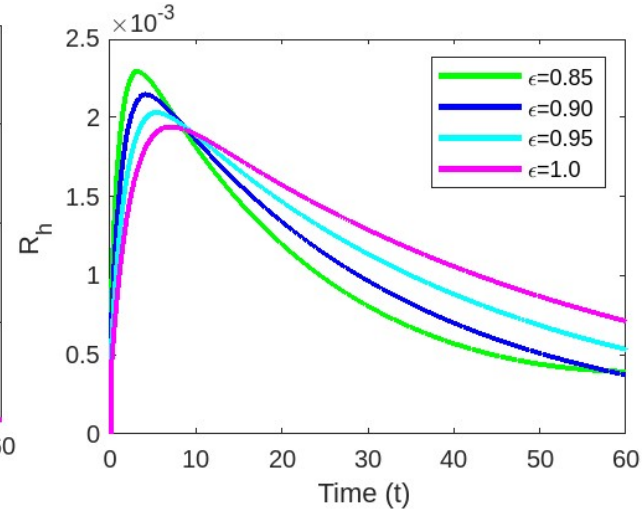

FIGURE 13. *

(d) Fractional Recovered Population.

FIGURE 14. Combined Fractional Population Graphs.

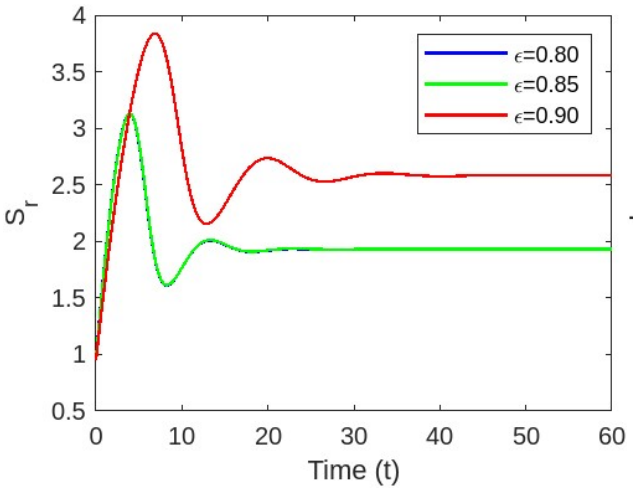

FIGURE 15. *
(a) Fractional Susceptible Rodents.

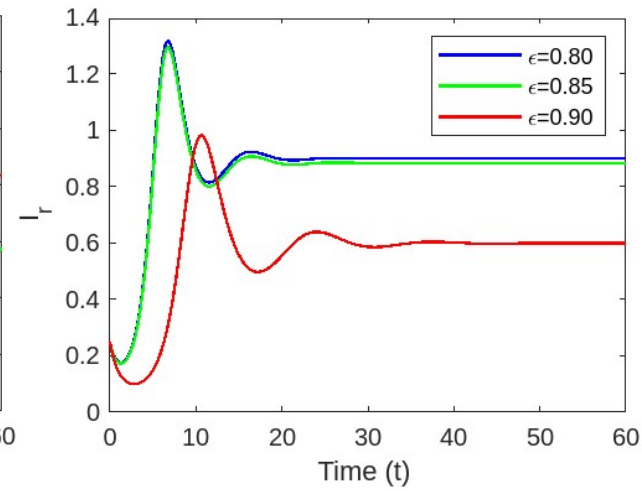

FIGURE 16. *
(b) Fractional Infected Rodents.

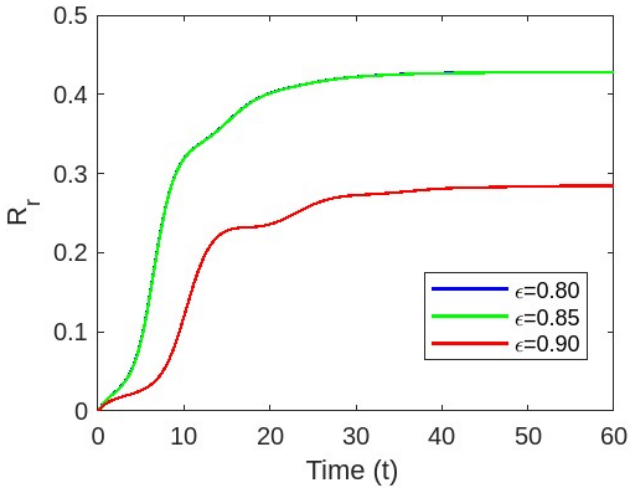

FIGURE 17. *
(c) Fractional Recovered Rodents.

FIGURE 18. Combined Fractional Rodent Populations.

8. Conclusions

This study uses fractal-fractional (FF) differential equations and the FF operator to explore a mathematical model for monkeypox virus transmission. Within the framework of the FFM derivative, fixed-point theory is employed to demonstrate the existence and uniqueness of solutions. Stability analysis is performed using the Ulam–Hyers method to confirm the required conditions. A two-step fractional Lagrange polynomial method is applied in conjunction with the FFM derivative to obtain numerical solutions. Simulations are carried out across different fractional orders and dimensions, followed by a brief discussion to assess the effectiveness of the numerical techniques. Future studies should focus on developing and evaluating additional epidemiological models based on FF differential equations for various infectious diseases. Comparing these models can provide significant insights into disease transmission and contribute to the design of more effective public health strategies.

Authors' contributions: T.G., S.M., M.S., I.A., and N.M. wrote the main manuscript text. All authors reviewed the manuscript.

Acknowledgment: The authors I. Ayoob and N. Mlaiki would like to thank Prince Sultan University for the support through the TAS research lab and for paying the APC.

Conflicts of Interest: The authors declare that there are no conflicts of interest regarding the publication of this paper.

References

[1] I.D. Ladnyj, P. Ziegler, E. Kima, A Human Infection Caused by Monkeypox Virus in Basankusu Territory, Democratic Republic of the Congo, Bull. World Health Organ. 46 (1972), 593–597.

[2] I. Arita, D.A. Henderson, Smallpox and Monkeypox in Non-Human Primates, Bull. World Health Organ. 39 (1968), 277.

[3] D.L. Heymann, M. Szczeniowski, K. Esteves, Re-emergence of Monkeypox in Africa: a Review of the Past Six Years, Br. Med. Bull. 54 (1998), 693–702. https://doi.org/10.1093/oxfordjournals.bmb.a011720.

[4] WHO, Monkeypox Fact Sheet, World Health Organization. https://www.who.int/news-room/fact-sheets/detail/monkeypox.

[5] C. Bhunu, S. Mushayabasa, J. Hyman, Modelling Hiv/aids and Monkeypox Co-Infection, Appl. Math. Comput. 218 (2012), 9504–9518. https://doi.org/10.1016/j.amc.2012.03.042.

[6] A.P. Lemos-Paião, C.J. Silva, D.F. Torres, An Epidemic Model for Cholera with Optimal Control Treatment, J. Comput. Appl. Math. 318 (2017), 168–180. https://doi.org/10.1016/j.cam.2016.11.002.

[7] E. Bonyah, M. Khan, K. Okosun, J. Gómez-Aguilar, On the Co-infection of Dengue Fever and Zika Virus, Optim. Control. Appl. Methods 40 (2019), 394–421. https://doi.org/10.1002/oca.2483.

[8] M. Suba, A. Venkatesan, T. Gunasekar, S. Manikandan, P. Raghavendran, S.S. Santra, S. Karmakar, Advancing Zika Virus Control with Fractional Order Optimal Control with Wolbachia-Infected Aedes Aegypti Mosquitoes, in: J. Singh, G.A. Anastassiou, D. Baleanu, D. Kumar (Eds.), Advances in Mathematical Modelling, Applied Analysis and Computation, Springer Nature Switzerland, Cham, 2025: pp. 160–183. https://doi.org/10.1007/978-3-031-90917-7_11.

[9] O. Makinde, K. Okosun, Impact of Chemo-Therapy on Optimal Control of Malaria Disease with Infected Immigrants, Biosystems 104 (2011), 32–41. https://doi.org/10.1016/j.biosystems.2010.12.010.

[10] E. Bonyah, K. Badu, S.K. Asiedu-Addo, Optimal Control Application to an Ebola Model, Asian Pac. J. Trop. Biomed. 6 (2016), 283–289. https://doi.org/10.1016/j.apjtb.2016.01.012.

[11] P.A. Naik, J. Zu, K.M. Owolabi, Global Dynamics of a Fractional Order Model for the Transmission of Hiv Epidemic with Optimal Control, Chaos, Solitons Fractals 138 (2020), 109826. https://doi.org/10.1016/j.chaos.2020.109826.

[12] K.S. Nisar, K. Logeswari, V. Vijayaraj, H.M. Baskonus, C. Ravichandran, Fractional Order Modeling the Gemini Virus in Capsicum Annuum with Optimal Control, Fractal Fract. 6 (2022), 61. https://doi.org/10.3390/fractalfract6020061.

[13] A. Atangana, Modelling the Spread of Covid-19 with New Fractal-Fractional Operators: Can the Lockdown Save Mankind Before Vaccination?, Chaos Solitons Fractals 136 (2020), 109860. https://doi.org/10.1016/j.chaos.2020.109860.

[14] X. Liu, S. Ahmad, M.U. Rahman, Y. Nadeem, A. Akgül, Analysis of a Tb and Hiv Co-Infection Model Under Mittag-Leffler Fractal-Fractional Derivative, Phys. Scr. 97 (2022), 054011. https://doi.org/10.1088/1402-4896/ac645e.

[15] S. Ahmad, A. Ullah, A. Akgül, M. De la Sen, Study of Hiv Disease and Its Association with Immune Cells Under Nonsingular and Nonlocal Fractal-fractional Operator, Complexity 2021 (2021), 1904067. https://doi.org/10.1155/2021/1904067.

[16] S. Etemad, B. Tellab, A. Zeb, S. Ahmad, A. Zada, S. Rezapour, H. Ahmad, T. Botmart, A Mathematical Model of Transmission Cycle of Cc-Hemorrhagic Fever Via Fractal–fractional Operators and Numerical Simulations, Results Phys. 40 (2022), 105800. https://doi.org/10.1016/j.rinp.2022.105800.

[17] Z. Ali, F. Rabiei, K. Shah, T. Khodadadi, Fractal-fractional Order Dynamical Behavior of an Hiv/aids Epidemic Mathematical Model, Eur. Phys. J. Plus 136 (2021), 36. https://doi.org/10.1140/epjp/s13360-020-00994-5.

[18] J. Kongson, C. Thaiprayoon, A. Neamvonk, J. Alzabut, W. Sudsutad, Investigation of Fractal-Fractional Hiv Infection by Evaluating the Drug Therapy Effect in the Atangana-Baleanu Sense, Math. Biosci. Eng. 19 (2022), 10762–10808. https://doi.org/10.3934/mbe.2022504.

[19] M. Farman, M. Amin, A. Akgül, A. Ahmad, M.B. Riaz, S. Ahmad, Fractal–fractional Operator for Covid-19 (omicron) Variant Outbreak with Analysis and Modeling, Results Phys. 39 (2022), 105630. https://doi.org/10.1016/j.rinp.2022.105630.

[20] A. Boukhouima, K. Hattaf, E.M. Lotfi, M. Mahrouf, D.F. Torres, N. Yousfi, Lyapunov Functions for Fractional-Order Systems in Biology: Methods and Applications, Chaos, Solitons Fractals 140 (2020), 110224. https://doi.org/10.1016/j.chaos.2020.110224.

[21] M. Amin, M. Farman, A. Akgül, R.T. Alqahtani, Effect of Vaccination to Control Covid-19 with Fractal Fractional Operator, Alex. Eng. J. 61 (2022), 3551–3557. https://doi.org/10.1016/j.aej.2021.09.006.

[22] H. Khan, F. Ahmad, O. Tunç, M. Idrees, On Fractal-Fractional Covid-19 Mathematical Model, Chaos, Solitons Fractals 157 (2022), 111937. https://doi.org/10.1016/j.chaos.2022.111937.

[23] T. Gunasekar, S. Manikandan, S. Haque, M. Suba, N. Mlaiki, Fractal-fractional Mathematical Modeling of Monkeypox Disease and Analysis of Its Ulam–hyers Stability, Bound. Value Probl. 2025 (2025), 20. https://doi.org/10.1186/s13661-025-02013-x.

[24] T. Gunasekar, S. Manikandan, M. Suba, A. Akgül, A Fractal-Fractional Mathematical Model for Covid-19 and Tuberculosis Using Atangana–baleanu Derivative, Math. Comput. Model. Dyn. Syst. 30 (2024), 857–881. https://doi.org/10.1080/13873954.2024.2426608.

[25] S. Manikandan, T. Gunasekar, A. Kouidere, K.A. Venkatesan, K. Shah, T. Abdeljawad, Mathematical Modelling of Hiv/aids Treatment Using Caputo–fabrizio Fractional Differential Systems, Qual. Theory Dyn. Syst. 23 (2024), 149. https://doi.org/10.1007/s12346-024-01005-z.

[26] H. Khan, K. Alam, H. Gulzar, S. Etemad, S. Rezapour, A Case Study of Fractal-Fractional Tuberculosis Model in China: Existence and Stability Theories Along with Numerical Simulations, Math. Comput. Simul. 198 (2022), 455–473. https://doi.org/10.1016/j.matcom.2022.03.009.

[27] T. Gunasekar, S. Manikandan, V. Govindan, P. D, J. Ahmad, W. Emam, I. Al-Shbeil, Symmetry Analyses of Epidemiological Model for Monkeypox Virus with Atangana–baleanu Fractional Derivative, Symmetry 15 (2023), 1605. https://doi.org/10.3390/sym15081605.